7
Fluidization

7.1 FUNDAMENTALS

When a fluid is passed upwards through a bed of particles the pressure loss in the fluid due to frictional resistance increases with increasing fluid flow. A point is reached when the upward drag force exerted by the fluid on the particles is equal to the apparent weight of particles in the bed. At this point the particles are lifted by the fluid, the separation of the particles increases, and the bed becomes fluidized. The force balance across the fluidized bed dictates that the fluid pressure loss across the bed of particles is equal to the apparent weight of the particles per unit area of the bed. Thus:

$$\text{pressure drop} = \frac{\text{weight of particles} - \text{upthrust on particle}}{\text{bed cross-sectional area}}$$

For a bed of particles of density ρ_p, fluidized by a fluid of density ρ_f to form a bed of depth H and voidage ε in a vessel of cross-sectional area A:

$$\Delta p = \frac{HA(1-\varepsilon)(\rho_p - \rho_f)g}{A} \tag{7.1}$$

or

$$\Delta p = H(1-\varepsilon)(\rho_p - \rho_f)g \tag{7.2}$$

A plot of fluid pressure loss across the bed versus superficial fluid velocity through the bed would have the appearance of Figure 7.1. Referring to Figure 7.1, the straight line region OA is the packed bed region. Here the solid particles do not move relative to one another and their separation is constant. The pressure loss

Introduction to Particle Technology, 2nd Edition Martin Rhodes
 ISBN: 978-0-470 -01427-1

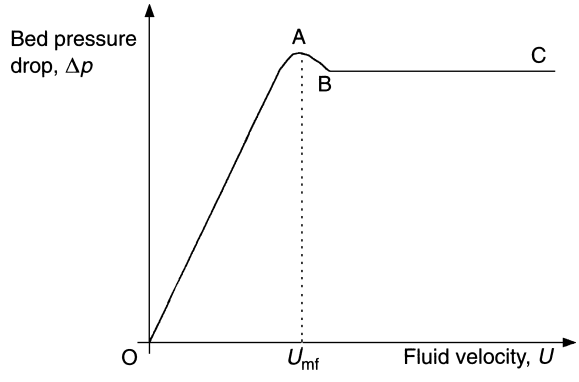

Figure 7.1 Pressure drop versus fluid velocity for packed and fluidized beds

versus fluid velocity relationship in this region is described by the Carman–Kozeny equation [Equation (6.9)] in the laminar flow regime and the Ergun equation in general [Equation (6.11)]. (See Chapter 6 for a detailed analysis of packed bed flow.)

The region BC is the fluidized bed region where Equation (7.1) applies. At point A it will be noticed that the pressure loss rises above the value predicted by Equation (7.1). This rise is more marked in small vessels and in powders which have been compacted to some extent before the test and is associated with the extra force required to overcome wall friction and adhesive forces between bed and the distributor.

The superficial fluid velocity at which the packed bed becomes a fluidized bed is known as the minimum fluidization velocity, U_{mf}. This is also sometimes referred to as the velocity at incipient fluidization (incipient meaning beginning). U_{mf} increases with particle size and particle density and is affected by fluid properties. It is possible to derive an expression for U_{mf} by equating the expression for pressure loss in a fluidized bed [Equation (7.2)] with the expression for pressure loss across a packed bed. Thus recalling the Ergun equation [Equation (6.11)]:

$$\frac{(-\Delta p)}{H} = 150\frac{(1-\varepsilon)^2}{\varepsilon^3}\frac{\mu U}{x_{sv}^2} + 1.75\frac{(1-\varepsilon)}{\varepsilon^3}\frac{\rho_f U^2}{x_{sv}} \tag{7.3}$$

substituting the expression for $(-\Delta p)$ from Equation (7.2):

$$(1-\varepsilon)(\rho_p - \rho_f)g = 150\frac{(1-\varepsilon)^2}{\varepsilon^3}\frac{\mu U_{mf}}{x_{sv}^2} + 1.75\frac{(1-\varepsilon)}{\varepsilon^3}\frac{\rho_f U_{mf}^2}{x_{sv}} \tag{7.4}$$

Rearranging,

$$\begin{aligned}(1-\varepsilon)(\rho_p - \rho_f)g = {} & 150\frac{(1-\varepsilon)^2}{\varepsilon^3}\left(\frac{\mu^2}{\rho_f x_{sv}^3}\right)\left(\frac{U_{mf}x_{sv}\rho_f}{\mu}\right) \\ & + 1.75\frac{(1-\varepsilon)}{\varepsilon^3}\left(\frac{\mu^2}{\rho_f x_{sv}^3}\right)\left(\frac{U_{mf}^2 x_{sv}^2 \rho_f^2}{\mu^2}\right)\end{aligned} \tag{7.5}$$

and so

$$(1-\varepsilon)(\rho_p-\rho_f)g\left(\frac{\rho_f x_{sv}^3}{\mu^2}\right)=150\frac{(1-\varepsilon)^2}{\varepsilon^3}Re_{mf}+1.75\frac{(1-\varepsilon)}{\varepsilon^3}Re_{mf}^2 \tag{7.6}$$

or

$$Ar=150\frac{(1-\varepsilon)}{\varepsilon^3}Re_{mf}+1.75\frac{1}{\varepsilon^3}Re_{mf}^2 \tag{7.7}$$

where Ar is the dimensionless number known as the Archimedes number,

$$Ar=\frac{\rho_f(\rho_p-\rho_f)gx_{sv}^3}{\mu^2}$$

and Re_{mf} is the Reynolds number at incipient fluidization,

$$Re_{mf}=\left(\frac{U_{mf}x_{sv}\rho_f}{\mu}\right)$$

In order to obtain a value of U_{mf} from Equation (7.7) we need to know the voidage of the bed at incipient fluidization, $\varepsilon=\varepsilon_{mf}$. Taking ε_{mf} as the voidage of the packed bed, we can obtain a crude U_{mf}. However, in practice voidage at the onset of fluidization may be considerably greater than the packed bed voidage. A typical often used value of ε_{mf} is 0.4. Using this value, Equation (7.7) becomes

$$Ar=1406\,Re_{mf}+27.3\,Re_{mf}^2 \tag{7.8}$$

Wen and Yu (1966) produced an empirical correlation for U_{mf} with a form similar to Equation (7.8):

$$Ar=1652Re_{mf}+24.51Re_{mf}^2 \tag{7.9}$$

The Wen and Yu correlation is often expressed in the form:

$$Re_{mf}=33.7[(1+3.59\times10^{-5}Ar)^{0.5}-1] \tag{7.10}$$

and is valid for spheres in the range $0.01<Re_{mf}<1000$.

For gas fluidization the Wen and Yu correlation is often taken as being most suitable for particles larger than 100 μm, whereas the correlation of Baeyens and Geldart (1974), shown in Equation (7.11), is best for particles less than 100 μm.

$$U_{mf}=\frac{(\rho_p-\rho_f)^{0.934}g^{0.934}x_p^{1.8}}{1110\mu^{0.87}\rho_f^{0.066}} \tag{7.11}$$

7.2 RELEVANT POWDER AND PARTICLE PROPERTIES

The correct density for use in fluidization equations is the particle density, defined as the mass of a particle divided by its hydrodynamic volume. This is the volume 'seen' by the fluid in its fluid dynamic interaction with the particle and includes the volume of all the open and closed pores (see Figure 7.2):

$$\text{particle density} = \frac{\text{mass of particle}}{\text{hydrodynamic volume of particle}}$$

For non-porous solids, this is easily measured by a gas pycnometer or specific gravity bottle, but these devices should not be used for porous solids since they give the true or absolute density ρ_{abs} of the material of which the particle is made and this is not appropriate where interaction with fluid flow is concerned:

$$\text{absolute density} = \frac{\text{mass of particle}}{\text{volume of solids material making up the particle}}$$

For porous particles, the particle density ρ_p (also called apparent or envelope density) is not easy to measure directly although several methods are given in Geldart (1990). Bed density is another term used in connection with fluidized beds; bed density is defined as

$$\text{bed density} = \frac{\text{mass of particles in a bed}}{\text{volume occupied by particles and voids between them}}$$

For example, 600 kg of powder is fluidized in a vessel of cross-sectional area 1 m^2 and achieves a bed height of 0.5 m. What is the bed density?

Mass of particles in the bed $= 600\,\text{kg}$

Volume occupied by particles and voids $= 1 \times 0.5 = 0.5\,m^3$

Hence, bed density $= 600/0.5 = 1200\,\text{kg}/m^3$.

If the particle density of these solids is $2700\,\text{kg}/m^3$, what is the bed voidage?

Bed density ρ_B is related to particle density ρ_p and bed voidage ε by Equation (7.12):

$$\rho_B = (1 - \varepsilon)\rho_p \tag{7.12}$$

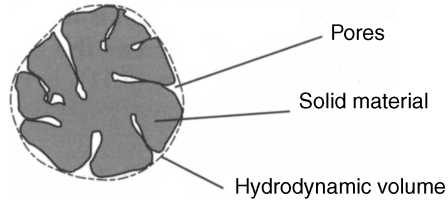

Figure 7.2 Hydrodynamic volume of a particle

Hence, voidage $= 1 - \dfrac{1200}{2700} = 0.555$.

Another density often used when dealing with powders is the bulk density. It is defined in a similar way to fluid bed density:

$$\text{bulk density} = \frac{\text{mass of particles}}{\text{volume occupied by particles and voids between them}}$$

The most appropriate particle size to use in equations relating to fluid–particle interactions is a hydrodynamic diameter, i.e. an equivalent sphere diameter derived from a measurement technique involving hydrodynamic interaction between the particle and fluid. In practice, however, in most industrial applications sizing is done using sieving and correlations use either sieve diameter, x_p or volume diameter, x_v. For spherical or near spherical particles x_v is equal to x_p. For angular particles, $x_v \approx 1.13x_p$.

For use in fluidization applications, starting from a sieve analysis the mean size of the powder is often calculated from

$$\text{mean } x_p = \frac{1}{\sum m_i/x_i} \tag{7.13}$$

where x_i is the arithmetic mean of adjacent sieves between which a mass fraction m_i is collected. This is the harmonic mean of the mass distribution, which was shown in Chapter 1 to be equivalent to the arithmetic mean of a surface distribution.

7.3 BUBBLING AND NON-BUBBLING FLUIDIZATION

Beyond the minimum fluidization velocity bubbles or particle-free voids may appear in the fluidized bed. Figure 7.3 shows bubbles in a gas fluidized bed. The

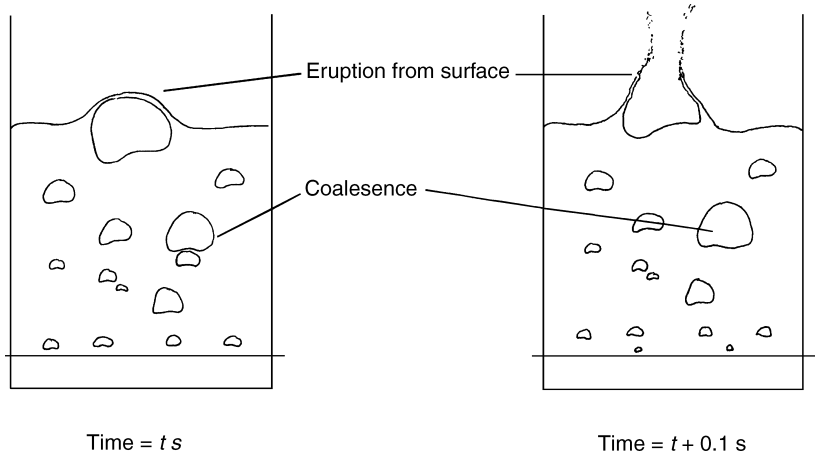

Figure 7.3 Sequence showing bubbles in a 'two-dimensional' fluidized bed of Group B powder. Sketches taken from video

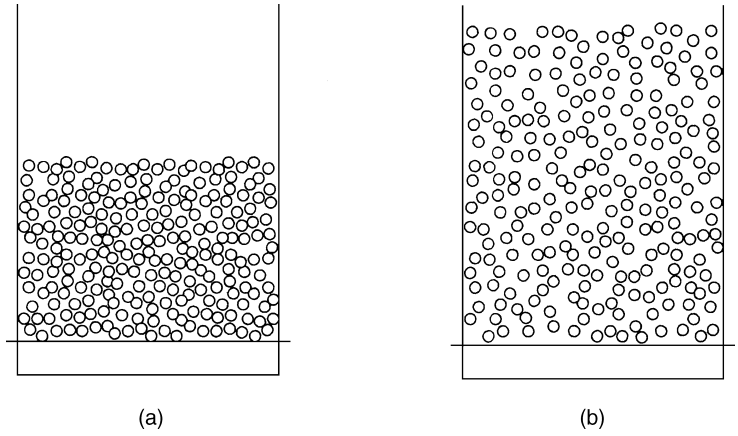

Figure 7.4 Expansion of a liquid fluidized bed: (a) just above U_{mf}; (b) liquid velocity several times U_{mf}. Note uniform increase in void fraciton. Sketches taken from video

equipment used Figure 7.3 is a so-called 'two-dimensional fluidized bed'. A favourite tool of researchers looking at bubble behaviour, this is actually a vessel of a rectangular cross-section, whose shortest dimension (into the page) is usually only 1 cm or so.

At superficial velocities above the minimum fluidization velocity, fluidization may in general be either bubbling or non-bubbling. Some combinations of fluid and particles give rise to *only bubbling* fluidization and some combinations give *only non-bubbling* fluidization. Most liquid fluidized systems, except those involving very dense particles, do not give rise to bubbling. Figure 7.4 shows a bed of glass spheres fluidized by water exhibiting non-bubbling fluidized bed behaviour. Gas fluidized systems, however, give either only bubbling fluidization or non-bubbling fluidization beginning at U_{mf}, followed by bubbling fluidization as fluidizing velocity increases. Non-bubbling fluidization is also known as particulate or homogeneous fluidization and bubbling fluidization is often referred to as aggregative or heterogeneous fluidization.

7.4 CLASSIFICATION OF POWDERS

Geldart (1973) classified powders into four groups according to their fluidization properties at ambient conditions. The Geldart classification of powders is now used widely in all fields of powder technology. Powders which when fluidized by air at ambient conditions give a region of non-bubbling fluidization beginning at U_{mf}, followed by bubbling fluidization as fluidizing velocity increases, are classified as Group A. Powders which under these conditions give only bubbling fluidization are classified as Group B. Geldart identified two further groups: Group C powders – very fine, cohesive powders which are incapable of fluidization in the strict sense, and Group D powders – large particles distinguished by their ability to produce deep spouting beds (see Figure 7.5). Figure 7.6 shows how the group classifications are related to the particle and gas properties.

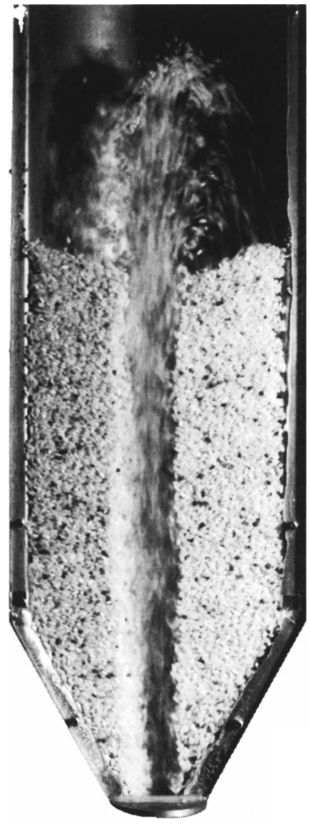

Figure 7.5 A spouted fluidized bed of rice

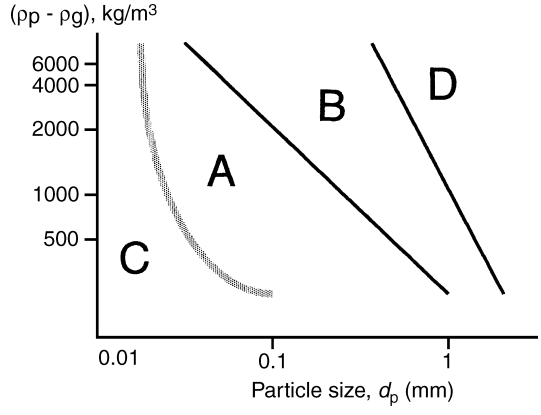

Figure 7.6 Simplified diagram showing Geldart's classification of powders according to their fluidization behaviour in air under ambient conditions (Geldart, 1973)

Table 7.1 Geldart's classification of powders

	Group C	Group A	Group B	Group D
Most obvious characteristic	Cohesive, difficult to fluidize	Ideal for fluidization. Exhibits range of non-bubbling fluidization	Starts bubbling at U_{mf}	Coarse solids
Typical solids	Flour, cement	Cracking catalyst	Building sand	Gravel, coffee beans
Property				
Bed expansion	Low because of chanelling	High	Moderate	Low
De-aeration rate	Initially fast, then exponential	Slow, linear	Fast	Fast
Bubble properties	No bubbles–only channels	Bubbles split and coalesce. Maximum bubble size	No limit to size	No limit to size
Solids mixing	Very low	High	Moderate	Low
Gas backmixing	Very low	High	Moderate	Low
Spouting	No	No	Only in shallow beds	Yes, even in deep beds

The fluidization properties of a powder in air may be predicted by establishing in which group it lies. It is important to note that at operating temperatures and pressures above ambient a powder may appear in a different group from that which it occupies at ambient conditions. This is due to the effect of gas properties on the grouping and may have serious implications as far as the operation of the fluidized bed is concerned. Table 7.1 presents a summary of the typical properties of the different powder classes.

Since the range of gas velocities over which non-bubbling fluidization occurs in Group A powders is small, bubbling fluidization is the type most commonly encountered in gas fluidized systems in commercial use. The superficial gas velocity at which bubbles first appear is known as the minimum bubbling velocity U_{mb}. Premature bubbling can be caused by poor distributor design or protuberances inside the bed. Abrahamsen and Geldart (1980) correlated the maximum values of U_{mb} with gas and particle properties using the following correlation:

$$U_{mb} = 2.07 \exp(0.716F) \left(\frac{x_p \rho_g^{0.06}}{\mu^{0.347}} \right) \tag{7.14}$$

where F is the fraction of powder less than 45 μm.

In Group A powders $U_{mb} > U_{mf}$, bubbles are constantly splitting and coalescing, and a maximum stable bubble size is achieved. This makes for good quality,

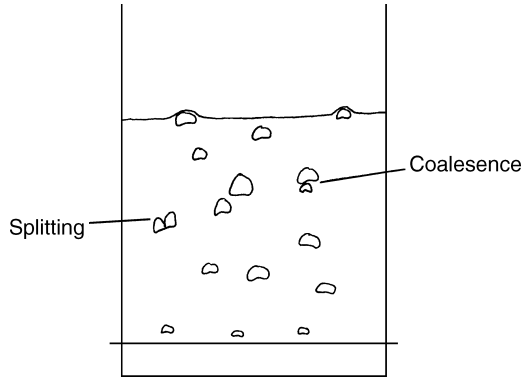

Figure 7.7 Bubbles in a 'two-dimensional' fluidized bed of Group A powder. Sketch taken from video

smooth fluidization. Figure 7.7 shows bubbles in a Group A powder in a two-dimensional fluidized bed.

In Groups B and D powders $U_{mb} = U_{mf}$, bubbles continue to grow, never achieving a maximum size (see Figure 7.3). This makes for rather poor quality fluidization associated with large pressure fluctuations.

In Group C powders the interparticle forces are large compared with the inertial forces on the particles. As a result, the particles are unable to achieve the separation they require to be totally supported by drag and buoyancy forces and true fluidization does not occur. Bubbles, as such, do not appear; instead the gas flow forms channels through the powder (see Figure 7.8). Since the particles are not fully supported by the gas, the pressure loss across the bed is always less than apparent weight of the bed per unit cross-sectional area. Consequently, measurement of bed pressure drop is one means of detecting this Group C behaviour if visual observation is inconclusive. Fluidization, of sorts, can be achieved with the assistance of a mechanical stirrer or vibration.

When the size of the bubbles is greater than about one-third of the diameter of the equipment their rise velocity is controlled by the equipment and they become slugs of gas. Slugging is attended by large pressure fluctuations and so it is generally avoided in large units since it can cause vibration to the plant. Slugging is unlikely to occur at any velocity if the bed is sufficiently shallow. According to Yagi and Muchi (1952), slugging will not occur provided the following criterion is satisfied:

$$\left(\frac{H_{mf}}{D}\right) \leq \frac{1.9}{(\rho_p x_p)^{0.3}} \tag{7.15}$$

This criterion works well for most powders. If the bed is deeper than this critical height then slugging will occur when the gas velocity exceeds U_{ms} as given by (Baeyens and Geldart, 1974):

$$U_{ms} = U_{mf} + 0.16(1.34D^{0.175} - H_{mf})^2 + 0.07(gD)^{0.5} \tag{7.16}$$

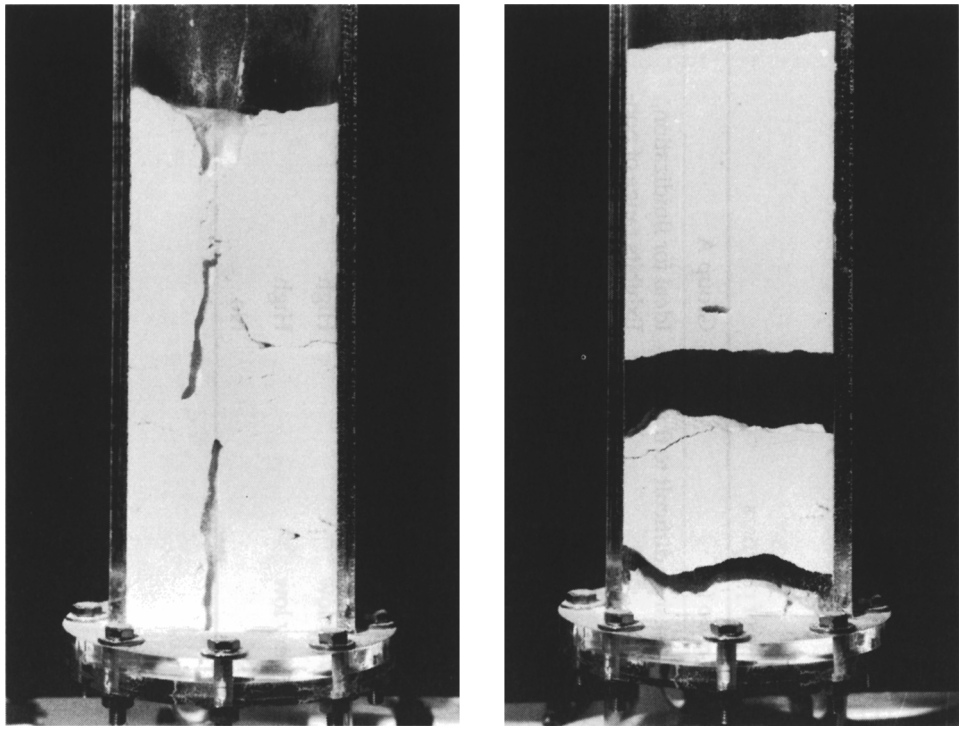

Figure 7.8 Attempts to fluidize Group C powder producing cracks and channels or discrete solid plugs

7.5 EXPANSION OF A FLUIDIZED BED

7.5.1 Non-bubbling Fluidization

In a non-bubbling fluidized bed beyond U_{mf} the particle separation increases with increasing fluid superficial velocity whilst the pressure loss across the bed remains constant. This increase in bed voidage with fluidizing velocity is referred to as bed expansion (see Figure 7.4). The relationship between fluid velocity and bed voidage may be determined by recalling the analysis of multiple particle systems (Chapter 3). For a particle suspension settling in a fluid under force balance conditions the relative velocity U_{rel} between particles and fluid is given by:

$$U_{rel} = U_p - U_f = U_T \varepsilon f(\varepsilon) \tag{7.17}$$

where U_p and U_f are the actual downward vertical velocities of the particles and the fluid, and U_T is the single particle terminal velocity in the fluid. In the case of a fluidized bed the time-averaged actual vertical particle velocity is zero ($U_p = 0$) and so

$$U_f = -U_T \varepsilon f(\varepsilon) \tag{7.18}$$

or

$$U_{fs} = -U_T \varepsilon^2 f(\varepsilon) \tag{7.19}$$

where U_{fs} is the downward volumetric fluid flux. In common with fluidization practice, we will use the term superficial velocity (U) rather than volumetric fluid flux. Since the upward superficial fluid velocity (U) is equal to the upward volumetric fluid flux $(-U_{fs})$, and $U_{fs} = U_f \varepsilon$, then:

$$U = U_T \varepsilon^2 f(\varepsilon) \tag{7.20}$$

Richardson and Zaki (1954) found the function $f(\varepsilon)$ which applied to both hindered settling and to non-bubbling fluidization. They found that in general, $f(\varepsilon) = \varepsilon^n$, where the exponent n was independent of particle Reynolds number at very low Reynolds numbers, when the drag force is independent of fluid density, and at high Reynolds number, when the drag force is independent of fluid viscosity, i.e.

$$\text{In general : } U = U_T \varepsilon^n \tag{7.21}$$

$$\text{For } Re_p \leq 0.3;\ f(\varepsilon) = \varepsilon^{2.65} \Rightarrow U = U_T \varepsilon^{4.65} \tag{7.22}$$

$$\text{For } Re_p \geq 500;\ f(\varepsilon) = \varepsilon^{0.4} \Rightarrow U = U_T \varepsilon^{2.4} \tag{7.23}$$

where Re_p is calculated at U_T.

Khan and Richardson (1989) suggested the correlation given in Equation (3.25) (Chapter 3) which permits the determination of the exponent n at intermediate values of Reynolds number (although it is expressed in terms of the Archimedes number Ar there is a direct relationship between Re_p and Ar). This correlation also incorporates the effect of the vessel diameter on the exponent. Thus Equations (7.21), (7.22) and (7.23) in conjunction with Equation (3.25) permit calculation of the variation in bed voidage with fluid velocity beyond U_{mf}. Knowledge of the bed voidage allows calculation of the fluidized bed height as illustrated below:

$$\text{mass of particles in the bed} = M_B = (1 - \varepsilon)\rho_p AH \tag{7.24}$$

If packed bed depth (H_1) and voidage (ε_1) are known, then if the mass remains constant the bed depth at any voidage can be determined:

$$(1 - \varepsilon_2)\rho_p AH_2 = (1 - \varepsilon_1)\rho_p AH_1 \tag{7.25}$$

hence

$$H_2 = \frac{(1 - \varepsilon_1)}{(1 - \varepsilon_2)} H_1$$

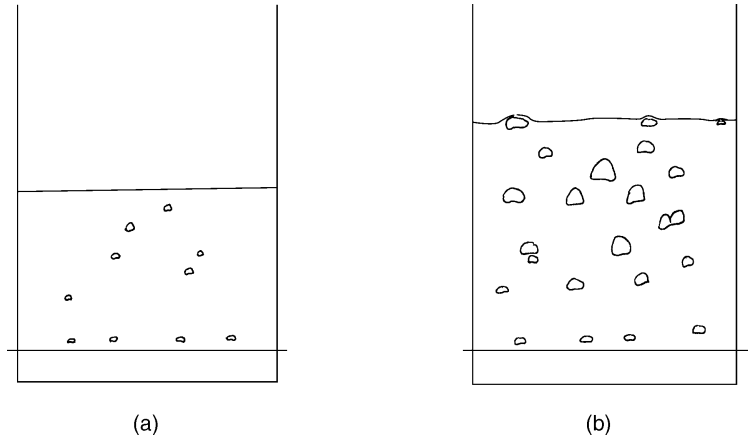

Figure 7.9 Bed expansion in a 'two-dimensional' fluidized bed of Group A powder: (a) just above U_{mb}; (b) fluidized at several times U_{mb}. Sketches taken from video

7.5.2 Bubbling Fluidization

The simplest description of the expansion of a bubbling fluidized bed is derived from the two-phase theory of fluidization of Toomey and Johnstone (1952). This theory considers the bubbling fluidized bed to be composed of two phases: the bubbling phase (the gas bubbles); and the particulate phase (the fluidized solids around the bubbles). The particulate phase is also referred to as the emulsion phase. The theory states that any gas in excess of that required at incipient fluidization will pass through the bed as bubbles. Figure 7.9 shows the effect of fluidizing gas velocity on bed expansion of a Group A powder fluidized by air. Thus, referring to Figure 7.10, Q is the actual gas flow rate to the fluid bed and Q_{mf} is the gas flow rate at incipient fluidization, then

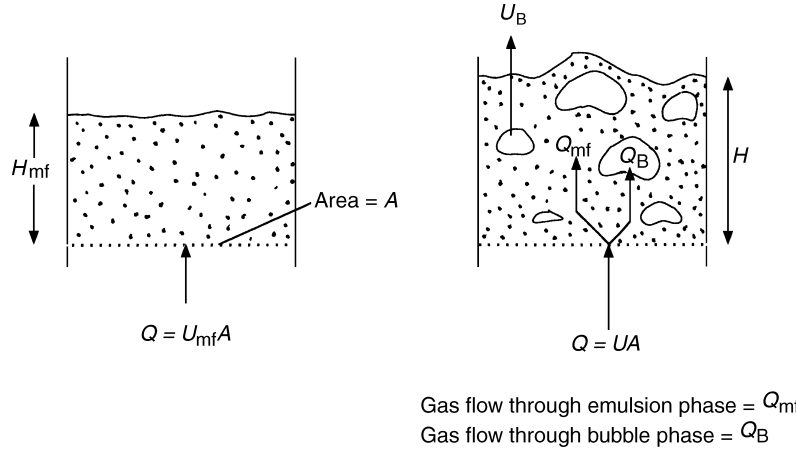

Figure 7.10 Gas flows in a fluidized bed according to the two-phase theory

gas passing through the bed as bubbles $= Q - Q_{mf} = (U - U_{mf})A$ (7.26)

gas passing through the emulsion phase $= Q_{mf} = U_{mf}A$ (7.27)

Expressing the bed expansion in terms of the fraction of the bed occupied by bubbles, ε_B:

$$\varepsilon_B = \frac{H - H_{mf}}{H} = \frac{Q - Q_{mf}}{AU_B} = \frac{(U - U_{mf})}{U_B} \tag{7.28}$$

where H is the bed height at U and H_{mf} is the bed height at U_{mf} and U_B is the mean rise velocity of a bubble in the bed (obtained from correlations; see below). The voidage of the emulsion phase is taken to be that at minimum fluidization ε_{mf}. The mean bed voidage is then given by:

$$(1 - \varepsilon) = (1 - \varepsilon_B)(1 - \varepsilon_{mf}) \tag{7.29}$$

In practice, the elegant two-phase theory overestimates the volume of gas passing through the bed as bubbles (the visible bubble flow rate) and better estimates of bed expansion may be obtained by replacing $(Q - Q_{mf})$ in Equation (7.28) with

$$\begin{aligned} \text{visible bubble flow rate}, Q_B &= YA(U - U_{mf}) \\ \text{where } 0.8 < Y < 1.0 &\text{ for Group A powders} \\ 0.6 < Y < 0.8 &\text{ for Group B powders} \\ 0.25 < Y < 0.6 &\text{ for GroupDpowders} \end{aligned} \tag{7.30}$$

Strictly the equations should be written in terms of U_{mb} rather than U_{mf} and Q_{mb} rather than Q_{mf}, so that they are valid for both Group A and Group B powders. Here they have been written in their original form. In practice, however, it makes little difference, since both U_{mb} and U_{mf} are usually much smaller than the superficial fluidizing velocity, U [so $(U - U_{mf}) \cong (U - U_{mb})$]. In rare cases where the operating velocity is not much greater than U_{mb}, then U_{mb} should be used in place of U_{mf} in the equations.

The above analysis requires a knowledge of the bubble rise velocity U_B, which depends on the bubble size d_{Bv} and bed diameter D. The bubble diameter at a given height above the distributor depends on the orifice density in the distributor N, the distance above the distributor L and the excess gas velocity $(U - U_{mf})$.

For Group B powders

$$d_{Bv} = \frac{0.54}{g^{0.2}}(U - U_{mf})^{0.4}(L + 4N^{-0.5})^{0.8} \text{ (Darton } et\ al.\text{, 1977)} \tag{7.31}$$

$$U_B = \Phi_B(g d_{Bv})^{0.5} \quad \text{(Werther,1983)} \tag{7.32}$$

where

$$\left\{\begin{array}{lll} \Phi_B = 0.64 & \text{for} & D \leq 0.1\,\text{m} \\ \Phi_B = 1.6D^{0.4} & \text{for} & 0.1 < D \leq 1\,\text{m} \\ \Phi_B = 1.6 & \text{for} & D > 1\,\text{m} \end{array}\right\} \tag{7.33}$$

For Group A powders

Bubbles reach a maximum stable size which may be estimated from

$$d_{\text{Bv max}} = 2(U_{T2.7})^2/g \text{ (Geldart, 1992)} \tag{7.34}$$

where $U_{T2.7}$ is the terminal free fall velocity for particles of diameter 2.7 times the actual mean particle diameter.

Bubble velocity for Group A powders is given by:

$$U_B = \Phi_A(gd_{Bv})^{0.5} \quad \text{(Werther, 1983)} \tag{7.35}$$

where

$$\left\{\begin{array}{lll} \Phi_A = 1 & \text{for} & D \leq 0.1\,\text{m} \\ \Phi_A = 2.5D^{0.4} & \text{for} & 0.1 < D \leq 1\,\text{m} \\ \Phi_A = 2.5 & \text{for} & D > 1\,\text{m} \end{array}\right\} \tag{7.36}$$

7.6 ENTRAINMENT

The term entrainment will be used here to describe the ejection of particles from the surface of a bubbling bed and their removal from the vessel in the fluidizing gas. In the literature on the subject other terms such as 'carryover' and 'elutriation' are often used to describe the same process. In this section we will study the factors affecting the rate of entrainment of solids from a fluidized bed and develop a simple approach to the estimation of the entrainment rate and the size distribution of entrained solids.

Consider a single particle falling under gravity in a static gas in the absence of any solids boundaries. We know that this particle will reach a terminal velocity when the forces of gravity, buoyancy and drag are balanced (see Chapter 2). If the gas of infinite extent is now considered to be moving upwards at a velocity equal to the terminal velocity of the particle, the particle will be stationary. If the gas is moving upwards in a pipe at a superficial velocity equal to the particle's terminal velocity, then:

(a) in laminar flow: the particle may move up or down depending on its radial position because of the parabolic velocity profile of the gas in the pipe.

(b) in turbulent flow: the particle may move up or down depending on its radial position. In addition the random velocity fluctuations superimposed on the time-averaged velocity profile make the actual particle motion less predictable.

If we now introduce into the moving gas stream a number of particles with a range of particle size some particles may fall and some may rise depending on their size and their radial position. Thus the entrainment of particles in an upward-flowing gas stream is a complex process. We can see that the rate of entrainment and the size distribution of entrained particles will in general depend on particle size and density, gas properties, gas velocity, gas flow regime–radial velocity profile and fluctuations and vessel diameter. In addition (i) the mechanisms by which the particles are ejected into the gas stream from the fluidized bed are dependent on the characteristics of the bed – in particular bubble size and velocity at the surface, and (ii) the gas velocity profile immediately above the bed surface is distorted by the bursting bubbles. It is not surprising then that prediction of entrainment from first principles is not possible and in practice an empirical approach must be adopted.

This empirical approach defines coarse particles as particles whose terminal velocities are greater than the superficial gas velocity ($U_T > U$) and fine particles as those for which $U_T < U$, and considers the region above the fluidized bed surface to be composed of several zones shown in Figure 7.11:

- *Freeboard*. Region between the bed surface and the gas outlet.

- *Splash zone*. Region just above the bed surface in which coarse particles fall back down.

- *Disengagement zone*. Region above the splash zone in which the upward flux and suspension concentration of fine particles decreases with increasing height.

- *Dilute-phase transport zone*. Region above the disengagement zone in which all particles are carried upwards; particle flux and suspension concentration are constant with height.

Note that, although in general fine particles will be entrained and leave the system and coarse particles will remain, in practice fine particles may stay in the system at velocities several times their terminal velocity and coarse particles may be entrained.

The height from the bed surface to the top of the disengagement zone is known as the transport disengagement height (TDH). Above TDH the entrainment flux and concentration of particles is constant. Thus, from the design point of view, in order to gain maximum benefit from the effect of gravity in the freeboard, the gas exit should be placed above the TDH. Many empirical correlations for TDH are available in the literature; those of Horio *et al*. (1980) presented in Equation (7.37)

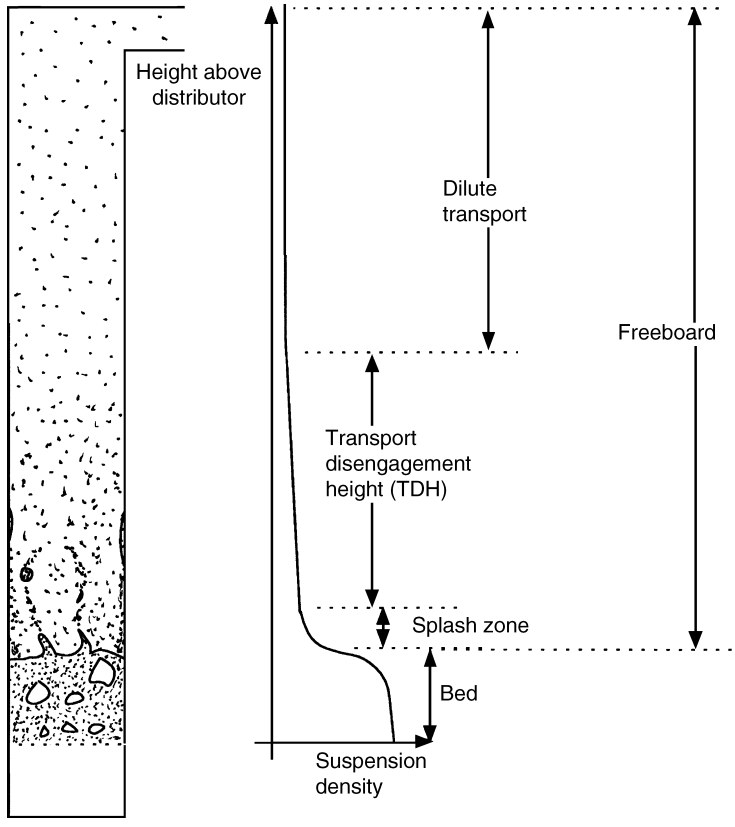

Figure 7.11 Zones in fluidized bed freeboard

and Zenz (1983) presented graphically in Figure 7.12 are two of the more reliable ones.

$$\mathrm{TDH} = 4.47 d_{\mathrm{bvs}}^{0.5} \tag{7.37}$$

Where d_{bvs} is the equivalent volume diameter of a bubble at the surface.

The empirical estimation of entrainment rates from fluidized beds is based on the following rather intuitive equation:

$$\begin{pmatrix}\text{instantaneous rate of loss}\\ \text{of solids of size } x_i\end{pmatrix} \propto \text{bed area} \times \begin{pmatrix}\text{fraction of bed with}\\ \text{size } x_i \text{ at time } t\end{pmatrix}$$
$$\text{i.e. } R_i = -\frac{\mathrm{d}}{\mathrm{d}t}(M_{\mathrm{B}} m_{\mathrm{B}i}) = K_{i\mathrm{h}}^{*} A m_{\mathrm{B}i} \tag{7.38}$$

where $K_{i\mathrm{h}}^{*}$ is the elutriation rate constant (the entrainment flux at height h above the bed surface for the solids of size x_i, when $m_{\mathrm{B}i} = 1.0$), M_{B} is the total mass of solids in the bed, A is the area of bed surface and $m_{\mathrm{B}i}$ is the fraction of the bed mass with size x_i at time t.

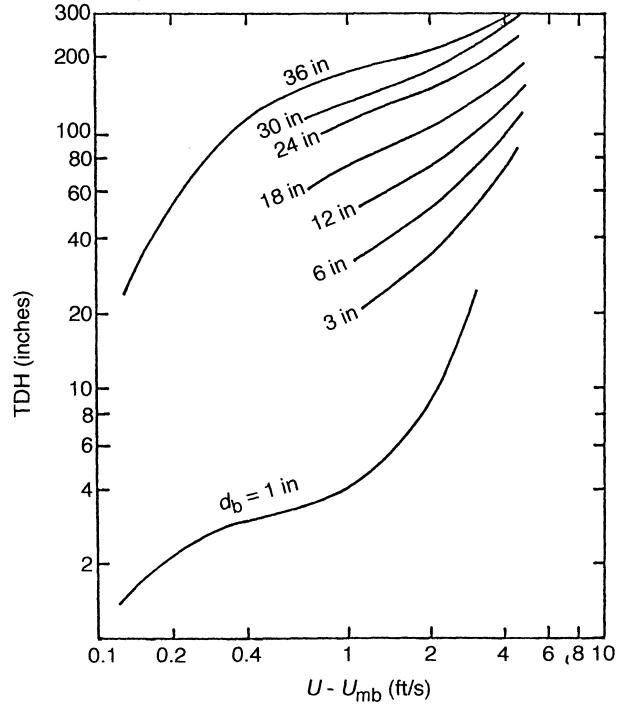

Figure 7.12 Graph for determination of transport disengagement height after the method of Zenz (1983). Reproduced by permission. [Note: TDH and the bubble diameter at the bubble surface d_b are given in inches (1 in. = 27.4 mm)]

For continuous operation, m_{Bi} and M_B are constant and so

$$R_i = K^*_{ih} A m_{Bi} \tag{7.39}$$

and

$$\text{total rate of entrainment, } R_T = \sum R_i = \sum K^*_{ih} A m_{Bi} \tag{7.40}$$

The solids loading of size x_i in the off-gases is $\rho_i = R_i/UA$ and the total solids loading of the gas leaving the freeboard is $\rho_T = \sum \rho_i$.

For batch operation, the rates of entrainment of each size range, the total entrainment rate and the particle size distribution of the bed change with time. The problem can best be solved by writing Equation (7.38) in finite increment form:

$$-\Delta(m_{Bi} M_B) = K^*_{ih} A m_{Bi} \Delta t \tag{7.41}$$

where $\Delta(m_{Bi} M_B)$ is the mass of solids in size range i entrained in time increment Δt.

$$\text{Total mass entrained in time } \Delta t = \sum_{i=1}^{k} [\Delta(m_{Bi} M_B)] \tag{7.42}$$

and mass of solids remaining in the bed at time

$$t + \Delta t = (M_B)_t - \sum_{i=1}^{k} [\Delta(m_{Bi} M_B)_t] \tag{7.43}$$

where subscript t refers to the value at time t.

$$\text{Bed composition at time } t + \Delta t = (m_{Bi})_{t+\Delta t} = \frac{(m_{Bi} M_B)_t - [\Delta(m_{Bi} M_B)_t]}{(M_B)_t - \sum_{i=1}^{k} \{\Delta(m_{Bi} M_B)_t\}} \tag{7.44}$$

Solution of a batch entrainment problem proceeds by sequential application of Equations (7.41)–(7.44) for the required time period.

The elutriation rate constant K_{ih}^* cannot be predicted from first principles and so it is necessary to rely on the available correlations which differ significantly in their predictions. Correlations are usually in terms of the carryover rate above TDH, $K_{i\infty}^*$. Two of the more reliable correlations are given below.

Geldart *et al*. (1979) (for particles $> 100\,\mu$m and $U > 1.2\,$m/s)

$$\frac{K_{i\infty}^*}{\rho_g U} = 23.7 \exp\left(-5.4 \frac{U_{Ti}}{U}\right) \tag{7.45}$$

Zenz and Weil (1958) (for particles $<100\,\mu$m and $U < 1.2\,$m/s)

$$\frac{K_{i\infty}^*}{\rho_g U} = \begin{cases} 1.26 \times 10^7 \left(\dfrac{U^2}{g x_i \rho_p^2}\right)^{1.88} & \text{when} \quad \left(\dfrac{U^2}{g x_i \rho_p^2}\right) < 3 \times 10^{-4} \\ 4.31 \times 10^4 \left(\dfrac{U^2}{g x_i \rho_p^2}\right)^{1.18} & \text{when} \quad \left(\dfrac{U^2}{g x_i \rho_p^2}\right) > 3 \times 10^{-4} \end{cases} \tag{7.46}$$

7.7 HEAT TRANSFER IN FLUIDIZED BEDS

The transfer of heat between fluidized solids, gas and internal surfaces of equipment is very good. This makes for uniform temperatures and ease of control of bed temperature.

7.7.1 Gas–Particle Heat Transfer

Gas to particle heat transfer coefficients are typically small, of the order of 5–20 $W \cdot m^2 K$. However, because of the very large heat transfer surface area provided by a mass of small particles (1 m^3 of 100 μm particles has a surface area of 60 000 m^2), the heat transfer between gas and particles is rarely limiting in fluid bed heat transfer. One of the most commonly used correlations for gas–particle heat transfer coefficient is that of Kunii and Levenspiel (1969):

$$Nu = 0.03 Re_p^{1.3} \quad (Re_p < 50) \tag{7.47}$$

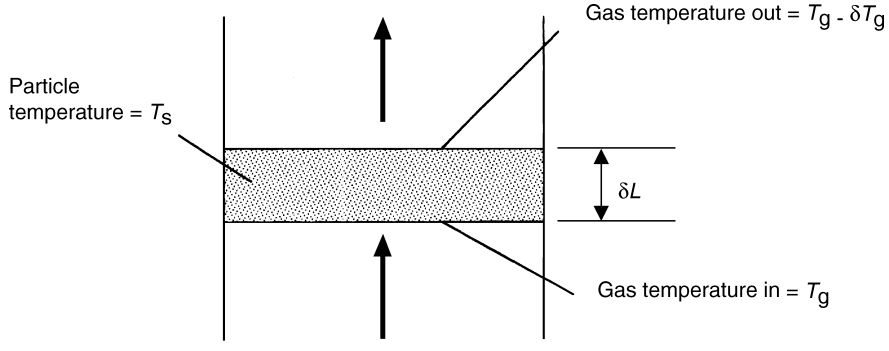

Figure 7.13 Analysis of gas–particle heat transfer in an element of a fluidized bed

where Nu is the Nusselt number $[h_{gp}x/k_g]$ and the single particle Reynolds number is based on the relative velocity between fluid and particle as usual.

Gas–particle heat transfer is relevant where a hot fluidized bed is fluidized by cold gas. The fact that particle–gas heat transfer presents little resistance in bubbling fluidized beds can be demonstrated by the following example:

Consider a fluidized bed of solids held at a constant temperature T_s. Hot fluidizing gas at temperature T_{g0} enters the bed. At what distance above the distributor is the difference between the inlet gas temperature and the bed solids temperature reduced to half its original value?

Consider an element of the bed of height δL at a distance L above the distributor (Figure 7.13). Let the temperature of the gas entering this element be T_g and the change in gas temperature across the element be δT_g. The particle temperature in the element is T_s.

The energy balance across the element gives

rate of heat loss by the gas = rate of heat transfer to the solids

that is

$$-(C_g U \rho_g) \mathrm{d}T_g = h_{gp} a (T_g - T_s) \mathrm{d}L \tag{7.48}$$

where a is the surface area of solids per unit volume of bed, C_g is the specific heat capacity of the gas, ρ_p is particle density, h_{gp} is the particle-to-gas heat transfer coefficient and U is superficial gas velocity.

Integrating with the boundary condition $T_g = T_{g0}$ at $L = 0$,

$$\ln\left(\frac{T_g - T_s}{T_{g0} - T_s}\right) = -\left(\frac{h_{gp} a}{U_{rel} \rho_g C_g}\right) L \tag{7.49}$$

The distance over which the temperature difference is reduced to half its initial value, $L_{0.5}$, is then

$$L_{0.5} = -\ln(0.5) \frac{C_g U_{rel} \rho_g}{h_{gp} a} = 0.693 \frac{C_g U_{rel} \rho_g}{h_{gp} a} \tag{7.50}$$

For a bed of spherical particles of diameter x, the surface area per unit volume of bed, $a = 6(1-\varepsilon)/x$, where ε is the bed voidage.

Using the correlation for h_{gp} in Equation (7.47), then

$$L_{0.5} = 3.85 \frac{\mu^{1.3} x^{0.7} C_g}{U_{rel}^{0.3} \rho_g^{0.3} (1-\varepsilon) k_g} \tag{7.51}$$

As an example we will take a bed of particles of mean size 100 μm, particle density 2500 kg/m^3, fluidized by air of density 1.2 kg/m^3, viscosity 1.84×10^{-5} Pa s, conductivity 0.0262 W/m/K and specific heat capacity 1005 J/kg/K.

Using the Baeyens equation for U_{mf} [Equation (7.11)], $U_{mf} = 9.3 \times 10^{-3}$m/s. The relative velocity between particles and gas under fluidized conditions can be approximated as U_{mf}/ε under these conditions.

Hence, assuming a fluidized bed voidage of 0.47, $U_{rel} = 0.02$ m/s.

Substituting these values in Equation (7.51), we find $L_{0.5} = 0.95$ mm. So, within 1 mm of entering the bed the difference in temperature between the gas and the bed will be reduced by half. Typically for particles less than 1 mm in diameter the temperature difference between hot bed and cold fluidizing gas would be reduced by half within the first 5 mm of the bed depth.

7.7.2 Bed–Surface Heat Transfer

In a bubbling fluidized bed the coefficient of heat transfer between bed and immersed surfaces (vertical bed walls or tubes) can be considered to be made up of three components which are approximately additive (Botterill, 1975).

$$\text{bed–surface heat transfer coefficient}, h = h_{pc} + h_{gc} + h_r$$

where h_{pc} is the particle convective heat transfer coefficient and describes the heat transfer due to the motion of packets of solids carrying heat to and from the surface, h_{gc} is the gas convective heat transfer coefficient describing the transfer of heat by motion of the gas between the particles and h_r is the radiant heat transfer coefficient. Figure 7.14, after Botterill (1986), gives an indication of the range of bed–surface heat transfer coefficients and the effect of particle size on the dominant heat transfer mechanism.

Particle convective heat transfer: On a volumetric basis the solids in the fluidized bed have about one thousand times the heat capacity of the gas and so, since the solids are continuously circulating within the bed, they transport the heat around the bed. For heat transfer between the bed and a surface the limiting factor is the gas conductivity, since all the heat must be transferred through a gas film between the particles and the surface (Figure 7.15). The particle–surface contact area is too small to allow significant heat transfer. Factors affecting the gas film thickness or the gas conductivity will therefore influence the heat transfer under particle convective conditions. Decreasing particle size, for example, decreases the mean gas film thickness and so improves h_{pc}. However, reducing particle size into the Group C range will reduce particle mobility and so reduce particle convective heat transfer. Increasing gas temperature increases gas conductivity and so improves h_{pc}.

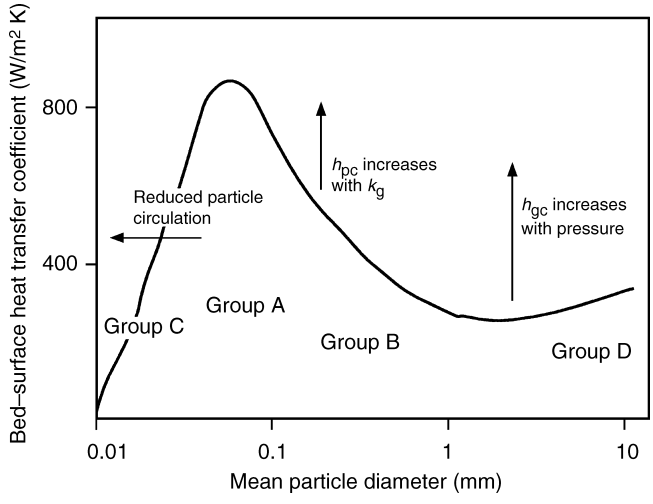

Figure 7.14 Range of bed–surface heat transfer coefficients

Particle convective heat transfer is dominant in Group A and B powders. Increasing gas velocity beyond minimum fluidization improves particle circulation and so increases particle convective heat transfer. The heat transfer coefficient increases with fluidizing velocity up to a broad maximum h_{max} and then declines as the heat transfer surface becomes blanketed by bubbles. This is shown in Figure 7.16 for powders in Groups A, B and D. The maximum in h_{pc} occurs relatively closer to U_{mf} for Group B and D powders since these powders give rise to bubbles at U_{mf} and the size of these bubbles increases with increasing gas velocity. Group A powders exhibit a non-bubbling fluidization between U_{mf} and U_{mb} and achieve a maximum stable bubble size.

Botterill (1986) recommends the Zabrodsky (1966) correlation for h_{max} for Group B powders:

$$h_{max} = 35.8 \frac{k_g^{0.6} \rho_p^{0.2}}{x^{0.36}} \quad \text{W/m}^2\text{/K} \tag{7.52}$$

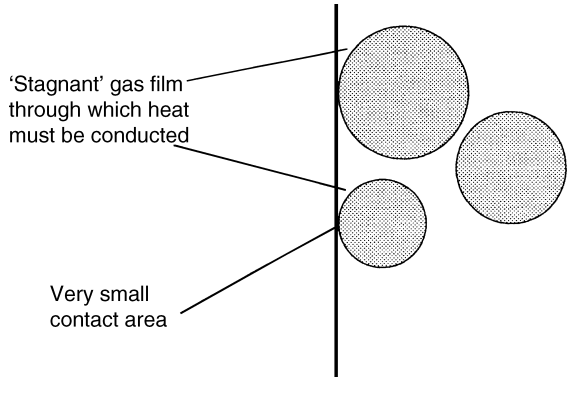

Figure 7.15 Heat transfer from bed particles to an immersed surface

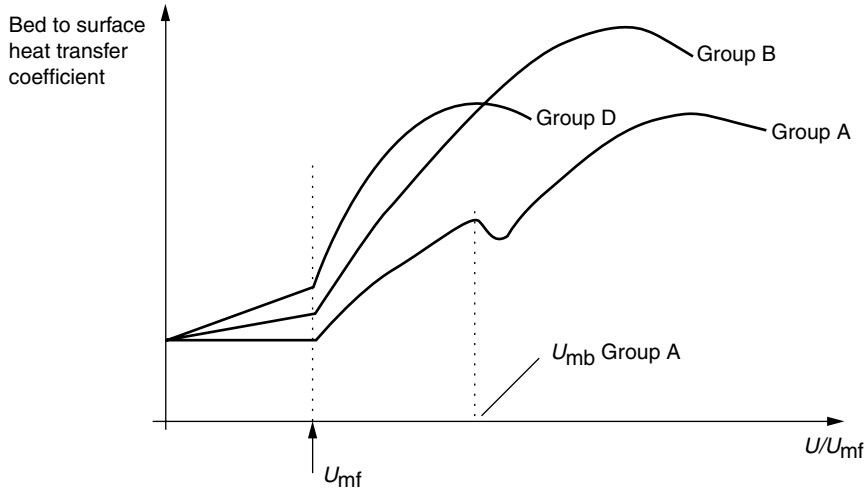

Figure 7.16 Effect of fluidizing gas velocity on bed–surface heat transfer coefficient in a fluidized bed

and the correlation of Khan *et al*. (1978) for Group A powders:

$$Nu_{max} = 0.157\,Ar^{0.475} \tag{7.53}$$

Gas convective heat transfer is not important in Group A and B powders where the flow of interstitial gas is laminar but becomes significant in Group D powders, which fluidize at higher velocities and give rise to transitional or turbulent flow of interstitial gas. Botterill suggests that the gas convective mechanism takes over from particle convective heat transfer as the dominant mechanism at $Re_{mf} \approx 12.5$ (Re_{mf} is the Reynolds number at minimum fluidization and is equivalent to an Archimedes number $Ar \approx 26\,000$). In gas convective heat transfer the gas specific heat capacity is important as the gas transports the heat around. Gas specific heat capacity increases with increasing pressure and in conditions where gas convective heat transfer is dominant, increasing operating pressure gives rise to an improved heat transfer coefficient h_{gc}. Botterill (1986) recommends the correlations of Baskakov and Suprun (1972) for h_{gc}.

$$Nu_{gc} = 0.0175\,Ar^{0.46}Pr^{0.33} \quad (\text{for } U > U_m) \tag{7.54}$$

$$Nu_{gc} = 0.0175 Ar^{0.46}Pr^{0.33}\left(\frac{U}{U_m}\right)^{0.3} \quad (\text{for } U_{mf} < U < U_m) \tag{7.55}$$

where U_m is the superficial velocity corresponding to the maximum overall bed heat transfer coefficient.

For temperatures beyond 600 °C radiative heat transfer plays an increasing role and must be accounted for in calculations. The reader is referred to Botterill (1986) or Kunii and Levenspiel (1990) for treatment of radiative heat transfer or for a more detailed look at heat transfer in fluidized beds.

7.8 APPLICATIONS OF FLUIDIZED BEDS

7.8.1 Physical Processes

Physical processes which use fluidized beds include drying, mixing, granulation, coating, heating and cooling. All these processes take advantage of the excellent mixing capabilities of the fluid bed. Good solids mixing gives rise to good heat transfer, temperature uniformity and ease of process control. One of the most important applications of the fluidized bed is to the drying of solids. Fluidized beds are currently used commercially for drying such materials as crushed minerals, sand, polymers, pharmaceuticals, fertilizers and crystalline products. The reasons for the popularity of fluidized bed drying are:

- The dryers are compact, simple in construction and of relatively low capital cost.
- The absence of moving parts, other than the feeding and discharge devices, leads to reliable operation and low maintenance.
- The thermal efficiency of these dryers is relatively high.
- Fluidized bed dryers are gentle in the handling of powders and this is useful when dealing with friable materials.

Fluidized bed granulation is dealt with in Chapter 13 and mixing is covered in Chapter 11. Fluidized beds are often used to cool particulate solids following a reaction. Cooling may be by fluidizing air alone or by the use of cooling water passing through tubes immersed in the bed (see Figure 7.17 for example). Fluidized beds are used for coating particles in the pharmaceutical and agricultural industries. Metal components may be plastic coated by dipping them hot into an air-fluidized bed of powdered thermosetting plastic.

7.8.2 Chemical Processes

The gas fluidized bed is a good medium in which to carry out a chemical reaction involving a gas and a solid. Advantages of the fluidized bed for chemical reaction include:

- The gas–solid contacting is generally good.
- The excellent solids circulation within the bed promotes good heat transfer between bed particles and the fluidizing gas and between the bed and heat transfer surfaces immersed in the bed.

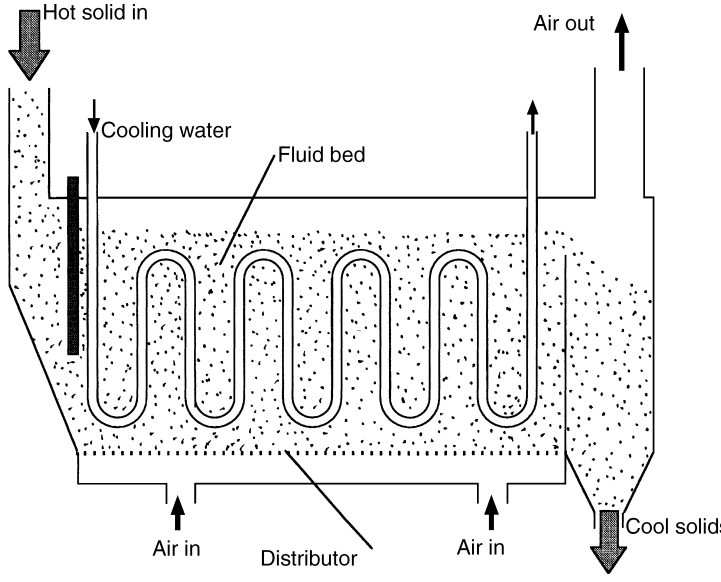

Figure 7.17 Schematic diagram of a fluidized bed solid cooler

- This gives rise to near isothermal conditions even when reactions are strongly exothermic or endothermic.
- The good heat transfer also gives rise to ease of control of the reaction.
- The fluidity of the bed makes for ease of removal of solids from the reactor.

However, it is far from ideal; the main problems arise from the two phase (bubbles and fluidized solids) nature of such systems. This problem is particularly acute where the bed solids are the catalyst for a gas-phase reaction. In such a case the ideal fluidized bed chemical reactor would have excellent gas–solid contacting, no gas by-passing and no back-mixing of the gas against the main direction of flow. In a bubbling fluidized bed the gas bypasses the solids by passing through the bed as bubbles. This means that unreacted reactants appear in the product. Also, gas circulation patterns within a bubbling fluidized bed are such that products are back-mixed and may undergo undesirable secondary reactions. These problems lead to serious practical difficulties particularly in the scaling-up of a new fluidized bed process from pilot plant to full industrial scale. This subject is dealt with in more detail in Kunii and Levenspiel (1990), Geldart (1986) and Davidson and Harrison (1971).

Figure 7.18 is a schematic diagram of one type of fluid catalytic cracking (FCC) unit, a celebrated example of fluidized bed technology for breaking down large molecules in crude oil to small molecules suitable for gasoline, etc. Other examples of the application of fluidized bed technology to different kinds of chemical reaction are shown in Table 7.2.

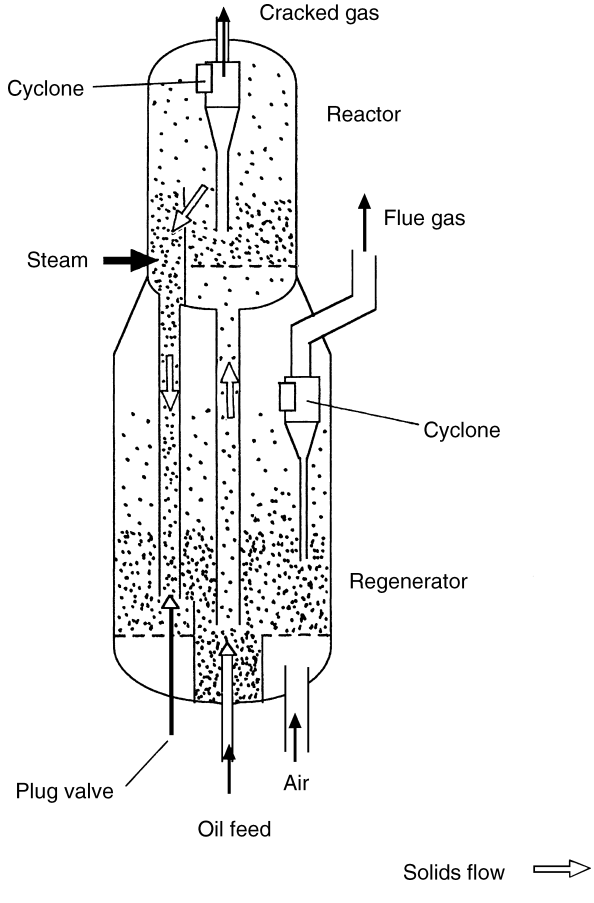

Figure 7.18 Kellogg's Model A Orthoflow FCC unit

Table 7.2 Summary of the types of gas–solid chemical reactions employing fluidization

Type	Example	Reasons for using a fluidized bed
Homogeneous gas-phase reactions	Ethylene hydrogenation	Rapid heating of entering gas. Uniform controllable temperature
Heterogeneous non-catalytic reactions	Sulfide ore roasting, combustion	Ease of solids handling. Temperature uniformity. Good heat transfer
Heterogeneous catalytic reactions	Hydrocarbon cracking, phthalic anhydride, acrylonitrile	Ease of solids handling. Temperature uniformity. Good heat transfer

7.9 A SIMPLE MODEL FOR THE BUBBLING FLUIDIZED BED REACTOR

In general, models for the fluidized bed reactor consider:

- the division of gas between the bubble phase and particulate phase;
- the degree of mixing in the particulate phase;
- the transfer of gas between the phases.

It is outside the scope of this chapter to review in detail the models available for the fluidized bed as a reactor. However, in order to demonstrate the key components of such models, we will use the simple model of Orcutt *et al*. (1962). Although simple, this model allows the key features of a fluidized bed reactor for gas-phase catalytic reaction to be explored.

The approach assumes the following:

- Original two-phase theory applies;
- Perfect mixing takes place in the particulate phase;
- There is no reaction in the bubble phase;

The model is one-dimensional and assumes steady state. The structure of the model is shown diagramatically in Figure 7.19. The following notation is used: C_0

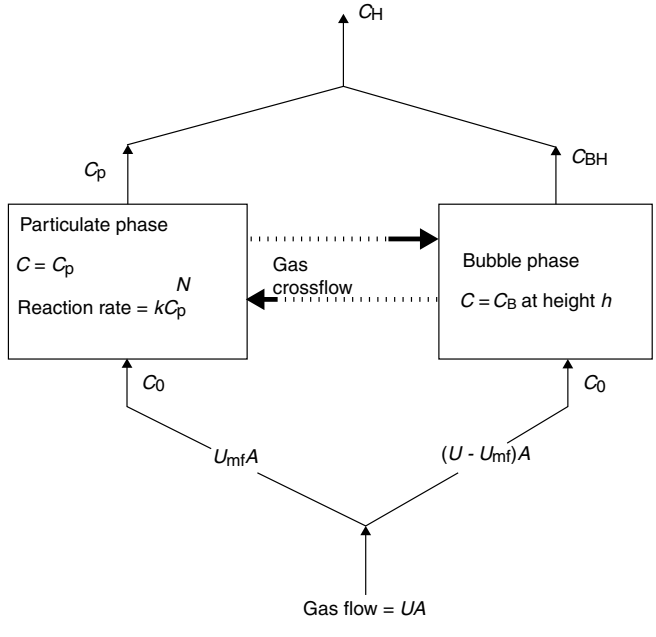

Figure 7.19 Schematic diagram of the Orcutt fluidized bed reactor model

is the concentration of reactant at distributor; C_p is the concentration of reactant in the particulate phase; C_B is the concentration of the reactant in the bubble phase at height h above the distributor; C_{BH} is the concentration of reactant leaving the bubble phase; and C_H is the concentration of reactant leaving the reactor.

In steady state, the concentration of reactant in the particulate phase is constant throughout the particulate phase because of the assumption of perfect mixing in the particulate phase. Throughout the bed, gaseous reactant is assumed to pass between particulate phase and bubble phase.
The overall mass balance on the reactant is:

$$\begin{pmatrix}\text{molar flow of}\\ \text{reactant into}\\ \text{reactor}\\ (1)\end{pmatrix} = \begin{pmatrix}\text{molar flow out}\\ \text{in the bubble phase}\\ (2)\end{pmatrix} + \begin{pmatrix}\text{molar flow out in}\\ \text{the particulate phase}\\ (3)\end{pmatrix} + \begin{pmatrix}\text{rate of}\\ \text{conversion}\\ (4)\end{pmatrix} \tag{7.56}$$

Term $(1) = UAC_0$

Term (2): molar reactant flow in bubble phase changes with height L above the distributor as gas is exchanged with the particulate phase. Consider an element of bed of thickness δL at a height L above the distributor. In this element:

$$\begin{pmatrix}\text{rate of increase of}\\ \text{reactant in bubble phase}\end{pmatrix} = \begin{pmatrix}\text{rate of transfer of}\\ \text{reactant from particulate phase}\end{pmatrix}$$
$$\text{i.e. } (U - U_{mf})A\delta C_B = -K_C(\varepsilon_B A\delta L)(C_B - C_p) \tag{7.57}$$

in the limit as $\delta L \to 0$,

$$\frac{dC_B}{dL} = -\frac{K_C\varepsilon_B(C_B - C_p)}{(U - U_{mf})} \tag{7.58}$$

where K_C is the mass transfer coefficient per unit bubble volume and ε_B is the bubble fraction. Integrating with the boundary condition that $C_B = C_0$ at $L_0 = 0$:

$$C_B = C_p + (C_0 - C_p)\exp\left(-\frac{K_C L}{U_B}\right) \tag{7.59}$$

since $\varepsilon_B = (U - U_{mf})/U_B$[Equation(7.28)].

At the surface of the bed, $L = H$ and so the reactant concentration in the bubble phase at the bed surface is given by:

$$C_{BH} = C_p + (C_0 - C_p)\exp\left(-\frac{K_C H}{U_B}\right) \tag{7.60}$$

Term $(2) = C_{BH}(U - U_{mf})A$

Term (3) $= U_{mf}AC_p$

Term (4): For a reaction which is jth order in the reactant under consideration,

$$\begin{pmatrix}\text{molar rate of conversion}\\ \text{per unit volume of solids}\end{pmatrix} = kC_p^j$$

where k is the reaction rate constant per unit volume of solids.
Therefore,

$$\begin{pmatrix}\text{molar rate of}\\ \text{conversion in bed}\end{pmatrix} = \begin{pmatrix}\text{molar rate of}\\ \text{conversion per unit}\\ \text{volume of solids}\end{pmatrix} \times \begin{pmatrix}\text{volume of solids}\\ \text{per unit volume of}\\ \text{particulate phase}\end{pmatrix} \times \begin{pmatrix}\text{volume of particulate}\\ \text{phase per unit}\\ \text{volume of bed}\end{pmatrix} \times \begin{pmatrix}\text{volume}\\ \text{of bed}\end{pmatrix}$$

hence, term (4),

$$\begin{pmatrix}\text{molar rate of}\\ \text{conversion in bed}\end{pmatrix} = kC_p^j(1-\varepsilon_p)(1-\varepsilon_B)AH \tag{7.61}$$

where ε_p is the particulate phase voidage.

Substituting these expressions for terms (1)–(4), the mass balance becomes:

$$\begin{aligned} UAC_0 = {} & \left[C_p + (C_0 - C_p)\exp\left(-\frac{K_C H}{U_B}\right)\right](U - U_{mf})A + U_{mf}AC_p \\ & + kC_p^j(1-\varepsilon_p)(1-\varepsilon_B)AH \end{aligned} \tag{7.62}$$

From this mass balance C_p may be found. The reactant concentration leaving the reactor C_H is then calculated from the reactant concentrations and gas flows through the bubble and particulate phases:

$$C_H = \frac{U_{mf}C_p + (U - U_{mf})C_{BH}}{U} \tag{7.63}$$

In the case of a first-order reaction ($j = 1$), solving the mass balance for C_p gives:

$$C_p = \frac{C_0[U - (U - U_{mf})e^{-\chi}]}{kH_{mf}(1-\varepsilon_p) + [U - (U - U_{mf})e^{-\chi}]} \tag{7.64}$$

where $\chi = K_C H/U_B$, equivalent to a number of mass transfer units for gas exchange between the phases. χ is related to bubble size and correlations are available. Generally χ decreases as bubble size increases and so small bubbles are preferred.

Thus from Equations (7.63) and (7.64), we obtain an expression for the conversion in the reactor:

$$1 - \frac{C_H}{C_0} = (1 - \beta e^{-\chi}) - \frac{(1 - \beta e^{-\chi})^2}{\dfrac{kH_{mf}(1 - \varepsilon_p)}{U} + (1 - \beta e^{-\chi})} \tag{7.65}$$

where $\beta = (U - U_{mf})/U$, the fraction of gas passing through the bed as bubbles. It is interesting to note that although the two-phase theory does not always hold, Equation (7.65) often holds with β still the fraction of gas passing through the bed as bubbles, but not equal to $(U - U_{mf})/U$.

Readers interested in reactions of order different from unity, solids reactions and more complex reactor models for the fluidized bed, are referred to Kunii and Levenspiel (1990).

Although the Orcutt model is simple, it does allow us to explore the effects of operating conditions, reaction rate and degree of interphase mass transfer on performance of a fluidized bed as a gas-phase catalytic reactor. Figure 7.20 shows the variation of conversion with reaction rate (expressed as $kH_{mf}(1 - \varepsilon_p/U)$) with excess gas velocity (expressed as β) calculated using Equation (7.65) for a first-order reaction.

Noting that the value of χ is dictated mainly by the bed hydrodynamics, we see that:

- *For slow reactions*, overall conversion is insensitive to bed hydrodynamics and so reaction rate k is the rate controlling factor.

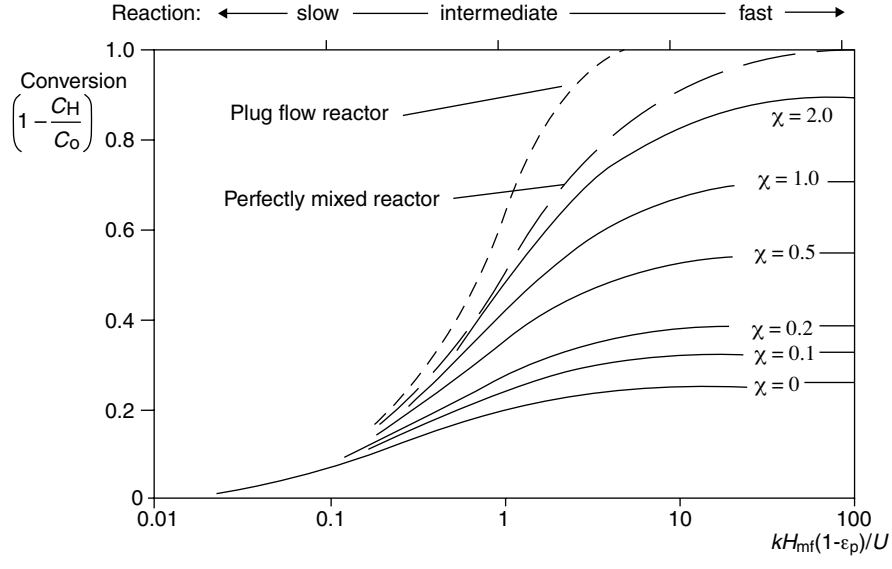

Figure 7.20 Conversion as a function of reaction rate and interphase mass transfer for $\beta = 0.75$ for a first-order gas phase catalytic reaction [based on Equation (7.65)]

- *For intermediate reactions*, both reaction rate and bed hydrodynamics affect the conversion.

- *For fast reactions*, the conversion is determined by the bed hydrodynamics.

These results are typical for a gas-phase catalytic reaction in a fluidized bed.

7.10 SOME PRACTICAL CONSIDERATIONS

7.10.1 Gas Distributor

The distributor is a device designed to ensure that the fluidizing gas is always evenly distributed across the cross-section of the bed. It is a critical part of the design of a fluidized bed system. Good design is based on achieving a pressure drop which is a sufficient fraction of the bed pressure drop. Readers are referred to Geldart (1986) for guidelines on distributor design. Many operating problems can be traced back to poor distributor design. Some distributor designs in common use are shown in Figure 7.21.

7.10.2 Loss of Fluidizing Gas

Loss of fluidizing gas will lead to collapse of the fluidized bed. If the process involves the emission of heat then this heat will not be dissipated as well from the packed bed as it was from the fluidized bed. The consequences of this should be considered at the design stage.

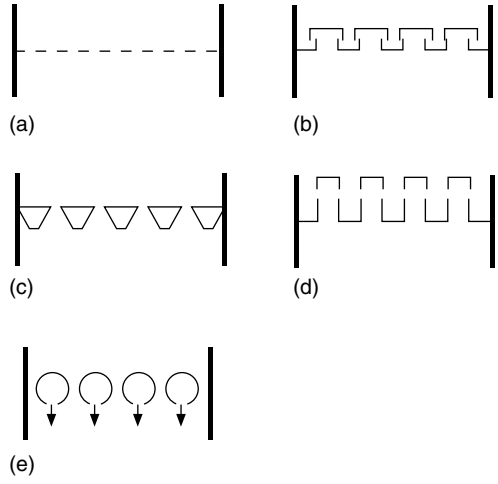

Figure 7.21 Some distributor designs in common use: (a) drilled plate; (b) cap design; (c) continuous horizontal slots; (d) standpipe design; (e) sparge tubes with holes pointing downwards

7.10.3 Erosion

All parts of the fluidized bed unit are subject to erosion by the solid particles. Heat transfer tubes within the bed or freeboard are particularly at risk and erosion here may lead to tube failure. Erosion of the distributor may lead to poor fluidization and areas of the bed becoming deaerated.

7.10.4 Loss of Fines

Loss of fine solids from the bed reduces the quality of fluidization and reduces the area of contact between the solids and the gas in the process. In a catalytic process this means lower conversion.

7.10.5 Cyclones

Cyclone separators are often used in fluidized beds for separating entrained solids from the gas stream (see Chapter 9). Cyclones installed within the fluidized bed vessel would be fitted with a dip-leg and seal in order to prevent gas entering the solids exit. Fluidized systems may have two or more stages of cyclone in series in order to improve separation efficiency. Cyclones are also the subject of erosion and must be designed to cope with this.

7.10.6 Solids Feeders

Various devices are available for feeding solids into the fluidized bed. The choice of device depends largely on the nature of the solids feed. Screw conveyors, spray feeders and pneumatic conveying are in common use.

7.11 WORKED EXAMPLES

WORKED EXAMPLE 7.1

3.6 kg of solid particles of density 2590 kg/m^3 and surface-volume mean size 748 μm form a packed bed of height 0.475 m in a circular vessel of diameter 0.0757 m. Water of density 1000 kg/m^3 and viscosity 0.001 Pa s is passed upwards through the bed. Calculate (a) the bed pressure drop at incipient fluidization, (b) the superficial liquid velocity at incipient fluidization, (c) the mean bed voidage at a superficial liquid velocity of 1.0 cm/s, (d) the bed height at this velocity and (e) the pressure drop across the bed at this velocity.

Solution

(a) Applying Equation (7.24) to the packed bed, we find the packed bed voidage:

$$\text{mass of solids} = 3.6 = (1-\varepsilon) \times 2590 \times \frac{\pi(0.0757)^2}{4} \times 0.475$$

hence, $\varepsilon = 0.3498$

Frictional pressure drop across the bed when fluidized:

$$(-\Delta p) = \frac{\text{weight of particles} - \text{upthrust on particles}}{\text{cross-sectional area}}$$

$$(-\Delta p) = \frac{Mg - Mg(\rho_f/\rho_p)}{A} \text{ (since upthrust = weight of fluid displaced by particles)}$$

$$\text{Hence, } (-\Delta p) = \frac{Mg}{A}\left(1 - \frac{\rho_f}{\rho_p}\right) = \frac{3.6 \times 9.81}{4.50 \times 10^{-3}}\left(1 - \frac{1000}{2590}\right) = 4817\,\text{Pa}$$

(b) Assuming that the voidage at the onset of fluidization is equal to the voidage of the packed bed, we use the Ergun equation to express the relationship between packed pressure drop and superficial liquid velocity:

$$\frac{(-\Delta p)}{H} = 3.55 \times 10^7 U^2 + 2.648 \times 10^6 U$$

Equating this expression for pressure drop across the packed bed to the fluidized bed pressure drop, we determine superficial fluid velocity at incipient fluidization, U_{mf}.

$$U_{mf} = 0.365 \text{ cm/s}$$

(c) The Richardson–Zaki equation [Equation (7.21)] allows us to estimate the expansion of a liquid fluidized bed.

$$U = U_T \varepsilon^n \qquad \text{[Equation(7.21)]}$$

Using the method given in Chapter 2, we determine the single particle terminal velocity, U_T.

$$Ar = 6527.9; \quad C_D Re_p^2 = 8704; \quad Re_p = 90; \quad U_T = 0.120 \text{ m/s}$$

Note that Re_p is calculated at U_T. At this value of Reynolds number, the flow is intermediate between viscous and inertial, and so we must use the correlation of Khan and Richardson [Equation (3.25)] to determine the exponent n in Equation (7.21):

$$\text{With } Ar = 6527.9, \; n = 3.202$$

Hence from Equation (7.21), $\varepsilon = 0.460$ when $U = 0.01$ m/s.

Mean bed voidage is 0.460 when the superficial liquid velocity is 1 cm/s.

(d) From Equation (7.25), we now determine the mean bed height at this velocity:

$$\text{Bed height(at } U = 0.01 \text{ m/s)} = \frac{(1 - 0.3498)}{(1 - 0.460)} 0.475 = 0.572\,\text{m}$$

(e) The frictional pressure drop across the bed remains essentially constant once the bed is fluidized. Hence at a superficial liquid velocity of 1 cm/s the frictional pressure drop across the bed is 4817 Pa.

However, the measured pressure drop across the bed will include the hydrostatic head of the liquid in the bed. Applying the mechanical energy equation between the bottom (1) and the top (2) of the fluidized bed:

$$\frac{p_1 - p_2}{\rho_f g} + \frac{U_1^2 - U_2^2}{2g} + (z_1 - z_2) = \text{friction head loss} = \frac{4817}{\rho_f g}$$
$$U_1 = U_2; \qquad z_1 - z_2 = -H = -0.572\,\text{m}$$

Hence, $p_1 - p_2 = 10\,428\,\text{Pa}$.

WORKED EXAMPLE 7.2

A powder having the size distribution given below and a particle density of 2500 kg/m^3 is fed into a fluidized bed of cross-sectional area 4 m^2 at a rate of 1.0 kg/s.

Size range number (i)	Size range (μm)	Mass fraction in feed
1	10–30	0.20
2	30–50	0.65
3	50–70	0.15

The bed is fluidized using air of density 1.2 kg/m^3 at a superficial velocity of 0.25 m/s. Processed solids are continuously withdrawn from the base of the fluidized bed in order to maintain a constant bed mass. Solids carried over with the gas leaving the vessel are collected by a bag filter operating at 100% total efficiency. None of the solids caught by the filter are returned to the bed. Assuming that the fluidized bed is well-mixed and that the freeboard height is greater than the transport disengagement height under these conditions, calculate at equilibrium:

(a) the flow rate of solids entering the filter bag;

(b) the size distribution of the solids in the bed;

(c) the size distribution of the solids entering the filter bag;

(d) the rate of withdrawal of processed solids from the base of the bed;

(e) the solids loading in the gas entering the filter.

Solution

First calculate the elutriation rate constants for the three size ranges under these conditions from the Zenz and Weil correlation [Equation (7.46)]. The value of particle size x used in the correlation is the arithmetic mean of each size range:

$$x_1 = 20 \times 10^{-6}\,\text{m}; \quad x_2 = 40 \times 10^{-6}\,\text{m}; \quad x_3 = 60 \times 10^{-6}\,\text{m}$$

$$\text{With } U = 0.25\,\text{m/s}, \rho_p = 2500\,\text{kg/m}^3 \quad \text{and} \quad \rho_f = 1.2\,\text{kg/m}^3$$
$$K^*_{1\infty} = 3.21 \times 10^{-2}\text{kg/m}^2\,\text{s}$$
$$K^*_{2\infty} = 8.74 \times 10^{-3}\text{kg/m}^2\,\text{s}$$
$$K^*_{3\infty} = 4.08 \times 10^{-3}\text{kg/m}^2\,\text{s}$$

Referring to Figure 7.W2.1 the overall and component material balances over the fluidized bed system are:

$$\text{Overall balance: } F = Q + R \tag{7W2.1}$$
$$\text{Component balance: } Fm_{F_i} = Qm_{Q_i} + Rm_{R_i} \tag{7W2.2}$$

where F, Q and R are the mass flow rates of solids in the feed, withdrawal and filter discharge, respectively, and m_{F_i}, m_{Q_i} and m_{R_i} are the mass fractions of solids in size range i in the feed, withdrawal and filter discharge, respectively.

From Equation (7.39) the entrainment rate of size range i at the gas exit from the freeboard is given by:

$$R_i = Rm_{R_i} = K^*_{i\infty} A m_{B_i} \tag{7W2.3}$$

and

$$R = \sum R_i = \sum Rm_{R_i} \tag{7W2.4}$$

Combining these equations with the assumption that the bed is well mixed ($m_{Q_i} = m_{B_i}$),

$$m_{B_i} = \frac{Fm_{F_i}}{F - R + K^*_{i\infty} A} \tag{7W2.5}$$

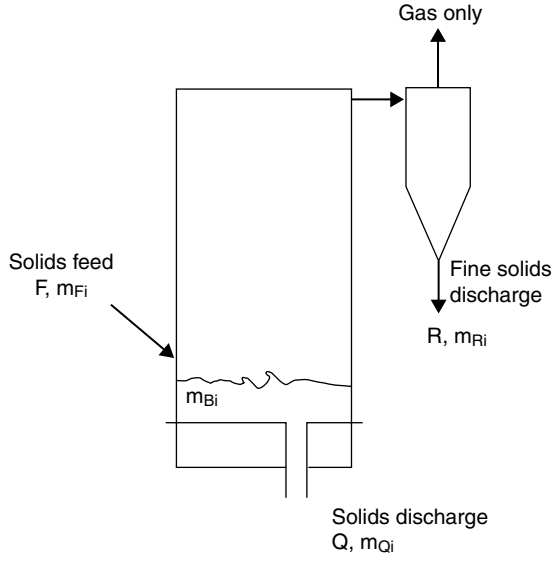

Figure 7W2.1 Schematic diagram showing solids flows and size distributions for the fluidized bed

Now both m_{B_i} and R are unknown. However, noting that $\sum m_{B_i} = 1$, we have

$$\frac{1.0 \times 0.2}{1.0 - R + (3.21 \times 10^{-2} \times 4)} + \frac{1.0 \times 0.65}{1.0 - R + (8.74 \times 10^{-3} \times 4)} + \frac{1.0 \times 0.15}{1.0 - R + (4.08 \times 10^{-3} \times 4)} = 1.0$$

Solving for R by trial and error, $R = 0.05\,\text{kg/s}$

(b) Substituting $R = 0.05\,\text{kg/s}$ in Equation (7W2.5), $m_{B_1} = 0.1855$, $m_{B_2} = 0.6599$ and $m_{B_3} = 0.1552$

Therefore size distribution of bed:

Size range number (i)	Size range (μm)	Mass fraction in bed
1	10–30	0.1855
2	30–50	0.6599
3	50–70	0.1552

(c) From Equation (7W2.3), knowing R and m_{B_i}, we can calculate m_{R_i}:

$$m_{R_i} = \frac{K^*_{1\infty} A m_{B_1}}{R} = \frac{3.21 \times 10^{-2} \times 4 \times 0.1855}{0.05} = 0.476$$

similarly, $m_{R_2} = 0.4614$, $m_{R_3} = 0.0506$

Therefore size distribution of solids entering filter:

Size range number (i)	Size range (μm)	Mass fraction entering filter
1	10–30	0.476
2	30–50	0.4614
3	50–70	0.0506

(d) From Equation (7W2.1), the rate of withdrawal of solids from the bed, $Q = 0.95\,\text{kg/s}$

(e) Solids loading for gas entering the filter,

$$\frac{\text{mass flow of solids}}{\text{volume flow of gas}} = \frac{R}{UA} = 0.05\,\text{kg/m}^3$$

WORKED EXAMPLE 7.3

A gas phase catalytic reaction is performed in a fluidized bed operating at a superficial gas velocity of 0.3 m/s. For this reaction under these conditions it is known that the reaction is first order in reactant A. The following information is given:

- bed height at incipient fluidization $= 1.5\,\text{m}$;
- operating mean bed height $= 1.65\,\text{m}$;
- voidage at incipient fluidization $= 0.47$;
- reaction rate constant $= 75.47$ (per unit volume of solids);
- $U_{\text{mf}} = 0.033\,\text{m/s}$;
- mean bubble rise velocity $= 0.111\,\text{m/s}$;
- mass transfer coefficient between bubbles and emulsion $= 0.1009$ (based on unit bubble volume) minimum fluidization velocity $= 0.033\,\text{m/s}$.

Use the reactor model of Orcutt *et al*. to determine:

(a) the conversion of reactant A;

(b) the effect on the conversion found in (a) of reducing the inventory of catalyst by one half;

(c) the effect on the conversion found in (a) of halving the bubble size (assuming the interphase mass transfer coefficient is inversely proportional to the square root of the bubble diameter).

Discuss your answers to (b) and (c) and state which mechanism is controlling conversion in the reactor.

Solution

(a) From Section 7.9 the model of Orcutt *et al*. gives for a first order reaction:

$$\text{conversion}, 1 - \frac{C_{\text{H}}}{C_0} = (1 - \beta e^{-\chi}) - \frac{(1 - \beta e^{-\chi})^2}{\frac{kH_{\text{mf}}(1 - \varepsilon_{\text{p}})}{U} + (1 - \beta e^{-\chi})} \qquad \text{[Equation(7.65)]}$$

where

$$\chi = \frac{K_{\text{C}} H}{U_{\text{B}}} \text{ and } \quad \beta = (U - U_{\text{mf}})/U$$

From the information given,

$$K_{\text{C}} = 0.1009,\ U_{\text{B}} = 0.111\ \text{m/s},\ U = 0.3\ \text{m/s},\ U_{\text{mf}} = 0.033\ \text{m/s},$$
$$H = 1.65\ \text{m},\ H_{\text{mf}} = 1.5\ \text{m},\ k = 75.47.$$

Hence, $\chi = 1.5$, $\beta = 0.89$ and $kH_{\text{mf}}(1 - \varepsilon_{\text{p}})/U = 200$ (assuming $\varepsilon_{\text{p}} = \varepsilon_{\text{mf}}$)

So, from Equation (7.65), conversion $= 0.798$.

(b) If the inventory of solids in the bed is halved, both the operating bed height H and the height at incipient fluidization H_{mf} are halved. Thus, assuming all else remains constant, under the new conditions

$$\chi = 0.75,\ \beta = 0.89 \text{ and } kH_{mf}(1 - \varepsilon_p)/U = 100$$

and so the new conversion $= 0.576$.

(c) If the bubble size is halved and K_C is proportional to $1/\sqrt{(\text{double diameter})}$,

$$\text{new } K_C = 1.414 \times 0.1009 = 0.1427$$

Hence, $\chi = 2.121$, giving conversion $= 0.889$.

(d) Comparing the conversion achieved in (c) with that achieved in (a), we see that improving interphase mass transfer has a significant effect on the conversion. We may also note that doubling the reaction rate (say by increasing the reactor temperature) and keeping everything else constant has a negligible effect on the conversion achieved in (a). We conclude, therefore, that under these conditions the transfer of gas between bubble phase and emulsion phase controls the conversion.

TEST YOURSELF

7.1 Write down the equation for the force balance across a fluidized bed and use it to come up with an expression for the pressure drop across a fluidized bed.

7.2 15 kg of particles of particle density 2000 kg/m^3 are fluidized in a vessel of cross-sectional area 0.03 m^2 by a fluid of density 900 kg/m^3. (a) What is the frictional pressure drop across the bed? (b) If the bed height is 0.6 m, what is the bed voidage?

7.3 Sketch a plot of pressure drop across a bed of powder versus velocity of the fluid flowing upwards through it. Include packed bed and fluidized bed regions. Mark on the incipient fluidization velocity.

7.4 What are the chief behaviour characteristics of the four Geldart powder groups?

7.5 What differentiates a Geldart Group A powder from a Geldart Group B powder?

7.6 According to Richardson and Zaki, how does bed voidage in a liquid-fluidized bed vary with fluidizing velocity at Reynolds numbers less than 0.3?

7.7 What is the basic assumption of the two-phase theory? Write down an equation that describes bed expansion as a function of superficial fluidizing velocity according to the two-phase theory.

7.8 Explain what is meant by particle convective heat transfer in a fluidized bed. In which Geldart group is particle convective heat transfer dominant?

7.9 Under what conditions does gas convective heat transfer play a significant role?

7.10 A fast gas phase catalytic reaction is performed in a fluidized bed using a particulate catalyst. Would conversion be increased by improving conditions for mass transfer between particulate phase and bubble phase?

EXERCISES

7.1 A packed bed of solid particles of density 2500 kg/m^3, occupies a depth of 1 m in a vessel of cross-sectional area 0.04 m^2. The mass of solids in the bed is 50 kg and the surface-volume mean diameter of the particles is 1 mm. A liquid of density 800 kg/m^2 and viscosity 0.002 Pa s flows upwards through the bed.

(a) Calculate the voidage (volume fraction occupied by voids) of the bed.

(b) Calculate the pressure drop across the bed when the volume flow rate of liquid is 1.44 m^3/h.

(c) Calculate the pressure drop across, the bed when it becomes fluidized.

[Answer: (a) 0.5; (b) 6560 Pa; (c) 8338 Pa.]

7.2 130 kg of uniform spherical particles with a diameter of 50 μm and particle density 1500 kg/m^3 are fluidized by water (density 1000 kg/m^3, viscosity 0.001 Pa s) in a circular bed of cross-sectional area 0.2 m^2. The single particle terminal velocity of the particles is 0.68 mm/s and the voidage at incipient fluidization is known to be 0.47.

(a) Calculate the bed height at incipient fluidization.

(b) Calculate the mean bed voidage when the liquid flow rate is 2×10^{-5} m^3/s.

[Answer: (a) 0.818 m; (b) 0.6622.]

7.3 130 kg of uniform spherical particles with a diameter of 60 μm and particle density 1500 kg/m^3 are fluidized by water (density 1000 kg/m^3, viscosity 0.001 Pa s) in a circular bed of cross-sectional area 0.2 m^2. The single particle terminal velocity of the particles is 0.98 mm/s and the voidage at incipient fluidization is known to be 0.47.

(a) Calculate the bed height at incipient fluidization.

(b) Calculate the mean fluidized bed voidage when the liquid flow rate is 2×10^{-5} m^3/s.

[Answer: (a) 0.818 m; (b) 0.6121.]

7.4 A packed bed of solid particles of density 2500 kg/m^3, occupies a depth of 1 m in a vessel of cross-sectional area 0.04 m^2. The mass of solids in the bed is 59 kg and the surface-volume mean diameter of the particles is 1 mm. A liquid of density 800 kg/m^3 and viscosity 0.002 Pa s flows upwards through the bed.

(a) Calculate the voidage (volume fraction occupied by voids) of the bed.

(b) Calculate the pressure drop across the bed when the volume flow rate of liquid is $0.72\ m^3/h$.

(c) Calculate the pressure drop across the bed when it becomes fluidized.

[Answer: (a) 0.41; (b) 7876 Pa; (c) 9839 Pa.]

7.5 12 kg of spherical resin particles of density $1200\ kg/m^3$ and uniform diameter 70 μm are fluidized by water (density $1000\ kg/m^3$ and viscosity 0.001 Pa s) in a vessel of diameter 0.3 m and form an expanded bed of height 0.25 m.

(a) Calculate the difference in pressure between the base and the top of the bed.

(b) If the flow rate of water is increased to $7\ cm^3/s$, what will be the resultant bed height and bed voidage (liquid volume fraction)?

State and justify the major assumptions.

[Answer: (a) Frictional pressure drop = 277.5 Pa, pressure difference = 2730 Pa; (b) height = 0.465 m; voidage = 0.696.]

7.6 A packed bed of solids of density $2000\ kg/m^3$ occupies a depth of 0.6 m in a cylindrical vessel of inside diameter 0.1 m. The mass of solids in the bed is 5 kg and the surface-volume mean diameter of the particles is 300 μm. Water (density $1000\ kg/m^3$ and viscosity 0.001 Pa s) flows upwards through the bed.

(a) What is the voidage of the packed bed?

(b) Use a force balance over the bed to determine the bed pressure drop when fluidized.

(c) Hence, assuming laminar flow and that the voidage at incipient fluidization is the same as the packed bed voidage, determine the minimum fluidization velocity. Verify the assumption of laminar flow.

[Answer: (a) 0.4692; (b) 3124 Pa; (c) 1.145 mm/s.]

7.7 A packed bed of solids of density $2000\ kg/m^3$ occupies a depth of 0.5 m in a cylindrical vessel of inside diameter 0.1 m. The mass of solids in the bed is 4 kg and the surface-volume mean diameter of the particles is 400 μm. Water (density 1000 kg and viscosity 0.001 Pa s) flows upwards through the bed.

(a) What is the voidage of the packed bed?

(b) Use a force balance over the bed to determine the bed pressure drop when fluidized.

(c) Hence, assuming laminar flow and that the voidage at incipient fluidization is the same as the packed bed voidage, determine the minimum fluidization velocity. Verify the assumption of laminar flow.

[Answer: (a) 0.4907; (b) 2498 Pa; (c) 2.43 mm/s.]

7.8 By applying a force balance, calculate the incipient fluidizing velocity for a system with particles of particle density 5000 kg/m^3 and mean volume diameter 100 μm and a fluid of density 1.2 kg/m^3 and viscosity 1.8×10^{-5} Pa s. Assume that the voidage at incipient fluidization is 0.5.

If in the above example the particle size is changed to 2 mm, what is U_{mf}?

[Answer: 0.045 m/s; 2.26 m/s.]

7.9 A powder of mean sieve size 60 μm and particle density 1800 kg/m^3 is fluidized by air of density 1.2 kg/m^3 and viscosity 1.84×10^{-5} Pa s in a circular vessel of diameter 0.5 m. The mass of powder charged to the bed is 240 kg and the volume flow rate of air to the bed is 140 m^3/h. It is known that the average bed voidage at incipient fluidization is 0.45 and correlation reveals that the average bubble rise velocity under the conditions in question is 0.8 m/s. Estimate:

(a) the minimum fluidization velocity, U_{mf};

(b) the bed height at incipient fluidization;

(c) the visible bubble flow rate;

(d) the bubble fraction;

(e) the particulate phase voidage;

(f) the mean bed height;

(g) the mean bed voidage.

[Answer: (a) Baeyens and Geldart correlation [Equation (7.11)], 0.0027 m/s; (b) 1.24 m; (c) 0.038 m^3/s (assumes $U_{mf} \cong U_{mb}$); (d) 0.245; (e) 0.45; (f) 1.64 m; (g) 0.585.]

7.10 A batch fluidized bed process has an initial charge of 2000 kg of solids of particle density 1800 kg/s^3 and with the size distribution shown below:

Size range number (i)	Size range (μm)	Mass fraction in feed
1	15–30	0.10
2	30–50	0.20
3	50–70	0.30
4	70–100	0.40

The bed is fluidized by a gas of density 1.2 kg/m^3 Pa s at a superficial gas velocity of 0.4 m/s.

The fluid bed vessel has a cross-sectional area of 1 m^2.

Using a discrete time interval calculation with a time increment of 5 min, calculate:

(a) the size distribution of the bed after 50 min;

(b) the total mass of solids lost from the bed in that time;

(c) the maximum solids loading at the process exit;

(d) the entrainment flux above the transport disengagement height of solids in size range 1 (15–30 μm) after 50 min.

Assume that the process exit is positioned above TDH and that none of the entrained solids are returned to the bed.

[Answer: (a) (range 1) 0.029, (2) 0.165, (3) 0.324, (4) 0.482; (b) 527 kg; (c) 0.514 kg/m^3 s; (d) 0.024 kg/m^2 s.]

7.11 A powder having a particle density of 1800 kg/m^3 and the following size distribution:

Size range number (i)	Size range (μm)	Mass fraction in feed
1	20–40	0.10
2	40–60	0.35
3	60–80	0.40
4	80–100	0.15

is fed into a fluidized bed 2 m in diameter at a rate of 0.2 kg/s. The cyclone inlet is 4 m above the distributor and the mass of solids in the bed is held constant at 4000 kg by withdrawing solids continuously from the bed. The bed is fluidized using dry air at 700 K (density 0.504 kg/m^3 and viscosity 3.33×10^{-5} Pa s) giving a superficial gas velocity of 0.3 m/s. Under these conditions the mean bed voidage is 0.55 and the mean bubble size at the bed surface is 5 cm. For this powder, under these conditions, $U_{mb} = 0.155$ cm/s.

Assuming that none of the entrained solids are returned to the bed, estimate:

(a) the flow rate and size distribution of the entrained solids entering the cyclone;

(b) the equilibrium size distribution of solids in the bed;

(c) the solids loading of the gas entering the cyclone;

(d) the rate at which solids are withdrawn from the bed.

[Answer: (a) 0.0485 kg/s, (range 1) 0.213, (2) 0.420, (3) 0.295, (4) 0.074; (b) (range 1) 0.0638, (2) 0.328, (3) 0.433, (4) 0.174; (c) 51.5 g/m^3; (d) 0.152 kg/s.]

7.12 A gas phase catalytic reaction is performed in a fluidized bed operating at a superficial gas velocity equivalent to $10 \times U_{mf}$. For this reaction under these conditions it is known that the reaction is first order in reactant A. Given the following information:

$$kH_{mf}(1 - \varepsilon_p)/U = 100;\ \chi = \frac{K_C H}{U_B} = 1.0$$

use the reactor model of Orcutt *et al.* to determine:

(a) the conversion of reactant A;

(b) the effect on the conversion found in (a) of doubling the inventory of catalyst;

(c) the effect on the conversion found in (a) of halving the bubble size by using suitable baffles (assuming the interphase mass transfer coefficient is inversely proportional to the bubble diameter).

If the reaction rate were two orders of magnitude smaller, comment on the wisdom of installing baffles in the bed with a view to improving conversion.

[Answer: (a) 0.6645; (b) 0.8744; (c) 0.8706.]